LPV/H∞Control of combined longitudinal/lateral dynamics of a small autonomous vehicle

Manel Betouche, Olivier Sename, Dario Penco, Pedro Kvieska

LPV/H_∞Control of combined longitudinal/lateral dynamics of a small autonomous vehicle

Manel BETOUCHE [*,**], **Olivier SENAME** [*],
Dario PENCO [**], **Pedro KVIESKA** [**]

[*] *Univ.Grenoble Alpes, CNRS, Grenoble INP, GIPSA-Lab, Grenoble, 38000,France{email: manel.betouche@grenoble-inp.fr, olivier.sename@grenoble-inp.fr}*
[**] *Ampere Software Technology - Renault Group - 1 avenue du Golf 78280 Guyancourt, France France {email: manel.betouche@ampere.cars, dario.penco@ampere.cars, pedro.kvieska@ampere.cars}*

Abstract:
This paper presents a novel LPV model for coupled longitudinal-lateral vehicle dynamics, enabling the design of LPV/H_∞ controllers using grid-based and polytopic methods. A comparative analysis evaluates their computational efficiency and control performance across varying driving conditions. The contributions include a combined LPV model, controller synthesis, and performance evaluation through simulations and real tests, demonstrating effective trajectory tracking for a scaled autonomous vehicle.

Keywords: Linear parameter-variation (LPV), H_∞ control, grid-based synthesis, polytopic approach, vehicle dynamics control, autonomous vehicle

1. INTRODUCTION

The study of vehicle dynamics is fundamental for understanding autonomous driving systems, as it ensures stability, safety, and optimal performance. While traditional methods often treat longitudinal and lateral dynamics separately, these dynamics are inherently coupled, particularly in high-speed maneuvers or complex driving scenarios. As highlighted in (Jazar 2017; Penco 2022), considering this coupling is essential for capturing the interactions that influence vehicle behavior. Therefore a combined modeling approach allows for a more comprehensive understanding of these dynamics, ensuring that both longitudinal and lateral effects are effectively addressed in advanced control systems.

On the other hand, nonlinear tire forces modeled through combined-slip representations (Pacejka 2006), offer realistic insights into vehicle behavior under extreme conditions such as high lateral acceleration maneuvers. These models highlight the significant coupling of longitudinal and lateral forces, particularly under varying road and driving conditions. Advanced control techniques, such as Model Predictive Control (MPC) (Li et al. 2021; Liu et al. 2024), sliding mode control (Teng et al. 2024), enhance stability and performance by managing the inherent non-linearities in tire dynamics.

In parallel, Linear Parameter-Varying (LPV) modeling has emerged as a powerful framework. LPV models, as described in (Apkarian and Gahinet 1995; Apkarian and Adams 1998; Blanchini et al. 2000; Sename et al. 2013), approximate nonlinear systems using parameter-dependent linear representations, enabling robust control methods such as H_∞ control. These models have been successfully applied to lateral vehicle dynamics, as demonstrated in (Kapsalis 2022; Atoui 2023), as well as integrated control systems (Doumiati et al. 2013), showcasing their adaptability to varying speed, road conditions, and driver inputs. As highlighted in (Fergani et al. 2016), LPV methods are also valuable in advanced applications like semi-active suspension control and complex vehicle dynamics modeling. By incorporating system variations and coupling effects, LPV techniques combine traditional linear methods with nonlinear complexities, providing an effective solution for modern vehicle control design.

Building on these foundations, this work proposes a novel LPV modeling approach to capture the combined longitudinal-lateral dynamics of vehicles. This allows for the development of advanced LPV/H_∞ controllers that address the coupling effects and non-linearities inherent in the vehicle dynamics. Two LPV synthesis techniques are considered: the grid-based approach and the polytopic approach. A comparative analysis evaluates these methods in terms of computational efficiency and control performance.

The main contributions of this paper are as follows:

- Development of a combined longitudinal-lateral vehicle LPV model, capturing essential non-linearities and coupling effects.
- Design and comparison of a MIMO LPV/H_∞ longitudinal/lateral controller through grid-based and polytopic approaches.

- Implementation of the grid-based control design on a small-scale autonomous vehicle, along with first experimental results.

The remainder of the paper is organized as follows: Section 2 describes the test platform used for the development of this work. Section 3 presents the vehicle dynamics model along with its LPV representation. The design of the LPV/H_∞ control synthesis methods is detailed in Section 4. Section 5 discusses the simulation results and provides a comparative analysis of the proposed approaches. Section 6 presents the experimental tests in the real world and the initial findings of the implementation of the proposed controllers. Finally, Section 7 concludes the paper with a summary of the findings and suggestions for future research directions.

2. EXPERIMENTAL PLATFORM

The test platform used in this work is located at the laboratory GIPSALab in Grenoble/France and is designed for evaluating control and planning algorithms for autonomous vehicles (see Fig. 1). It comprises a motion capture system, a scaled vehicle, and a monitoring interface, all working together to provide precise measurements and remote control.

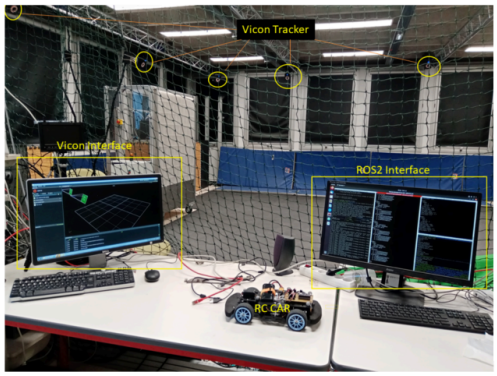

Fig. 1. Test platform

The motion capture system, based on Qualisys technology, utilizes infrared cameras to track the position and orientation of the vehicle through reflective markers. The system operates at a high acquisition frequency of 20 ms, ensuring smooth and accurate tracking. The scaled vehicle, capable of speeds up to 3 m/s, features actuators for longitudinal control (torque/speed) and lateral control (steering). A remote PC equipped with ROS2 and Simulink interfaces handles monitoring and control via WiFi, processing motion data and sending control commands. Offloading computational tasks to the PC ensures efficient execution of complex algorithms. This setup enables precise testing and validation of advanced control algorithms under varied conditions, ensuring performance under various scenarios as detailed in (Medero Borrell 2023) .

3. VEHICLE MODELING

3.1 Nonlinear Combined Model

The considered model is the commonly used bicycle model (see Kiencke et al. 2005), illustrated in Fig. 2, selected for its ability to accurately represent the dynamics of the vehicle in both lateral and longitudinal motions.

The model relies on the following assumptions:

- The vehicle is simplified as a rigid body with two effective wheels (front and rear) to capture key dynamics while reducing complexity.
- Aerodynamic and suspension effects, as well as rolling forces, are neglected due to their minimal influence in the testing platform described in Section 2.
- Nonlinear tire models are used to represent lateral and longitudinal forces, accounting for coupling and saturation during high-dynamic maneuvers.
- The actuators are subject to saturation limits, however, for simplicity, this aspect is not explicitly considered in the modeling.

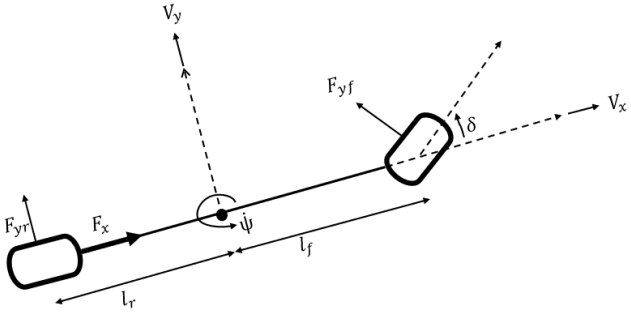

Fig. 2. Bicycle model of vehicle dynamics

Table of Notations

Symbol	Description
V_x	Longitudinal velocity [m/s]
V_y	Lateral velocity [m/s]
$\dot{\psi}$	Yaw rate [rad/s]
δ	Steering angle [rad]
ω	Wheel velocity [rad/s]
F_x	Longitudinal tire force [N]
F_{yf}	Front lateral tire force [N]
F_{yr}	Rear lateral tire force [N]
$C_\sigma(\cdot)$	Longitudinal stiffness coefficient
$C_{\alpha f}(\cdot)$	Front lateral stiffness coefficient
$C_{\alpha r}(\cdot)$	Rear lateral stiffness coefficient
m	Vehicle mass [kg]
l_f	Distance from CG to front axle [m]
l_r	Distance from CG to rear axle [m]
I_z	Yaw moment of inertia [kg·m^2]

Table 1. Table of notations used in the vehicle model.

The equations of motion describing the coupled longitudinal and lateral dynamics of the vehicle are as follows:

$$\begin{cases} \dot{V}_x = \frac{1}{m}(F_x - F_{yf}\sin\delta) + V_y\dot{\psi} \\ \dot{V}_y = \frac{1}{m}(F_{yf}\cos\delta + F_{yr}) - V_x\dot{\psi} \\ \ddot{\psi} = \frac{1}{I_z}(l_f F_{yf}\cos\delta - l_r F_{yr}) \end{cases} \tag{1}$$

$$\begin{cases} F_x = C_\sigma(.)(\frac{rw - V_x}{V_x}) \\ F_{yf} = C_{\alpha f}(.)(\delta - atan(\frac{(V_y + l_f\dot{\psi})}{V_x}) \\ F_{yr} = C_{\alpha r}(.)(-atan(\frac{(V_y - l_f\dot{\psi})}{V_x}) \end{cases} \quad (2)$$

In the linear model of tire forces, the stiffness coefficients $C_\star(\cdot)$ are typically assumed to be constant, whereas in the nonlinear model, they vary non-linearly for significant slip values. To capture this behavior in our platform presented in Section 2, and due to the absence of direct measurements of longitudinal and lateral slips, these coefficients have been modeled as nonlinear polynomial functions of the longitudinal velocity V_x, namely $C_\sigma(V_x)$, $C_{\alpha f}(V_x)$, and $C_{\alpha r}(V_x)$. This choice allows us to leverage the measurable longitudinal velocity for parameter identification, ensuring that the model adequately reflects variations in vehicle dynamics as a function of speed. Further details on this modeling approach can be found in (Medero Borrell 2023).

3.2 LPV Control Oriented Modeling

Nonlinear systems can be effectively represented using the state-space framework, which provides a structured approach for analyzing dynamic behaviors and designing advanced control strategies, as detailed in (Slotine et al. 1991). Generally, a nonlinear system can be expressed as:

$$\dot{x}(t) = f(x,u)x(t) + g(x,u)u(t), \quad (3)$$

where $x(t)$ represents the state vector, $u(t)$ is the input vector, and f, g are nonlinear functions capturing the system dynamics.

In this work, we apply this formulation to the vehicle dynamics model introduced in Section 3.1. The state vector is defined as $x(t) = [V_x, V_y, \dot{\psi}]^T$, where V_x and V_y are the longitudinal and lateral velocities, and $\dot{\psi}$ is the yaw rate. The input vector is $u(t) = [\delta, \omega]^T$, where δ denotes the steering angle, and ω represents the rotational speed of the wheel. Considering the small-angle approximation, where $\sin(\delta) \approx \delta$ and $\cos(\delta) \approx 1$, the system equations can be reformulated in state-space form as presented in Equation (4).

To make the model compatible with the chosen control method, which requires a linear structure, the nonlinear model is reformulated into a LPV framework, a widely studied approach in the literature (Leith et al. 2000; Toth 2010; Hoffmann et al. 2015). This reformulation encapsulates the non-linearities within the matrices A and B, which are functions of a parameter vector $\rho = [\rho_1, \rho_2, \ldots, \rho_n]^T$. This vector is both measurable and bounded, allowing the quasi-LPV state-space representation to be expressed as:

$$\dot{x}(t) = A(\rho)x(t) + B(\rho)u(t), \quad (5)$$

where $A(\rho)$ and $B(\rho)$ are parameter-dependent matrices. The scheduling parameters ρ_i are constrained within known bounds:

$$\rho_i^{\min} \leq \rho_i \leq \rho_i^{\max}, \quad \forall i \in \{1, 2, \ldots, n\}.$$

When the parameters ρ_i explicitly depend on the system's states or inputs, the resulting model is referred to as a quasi-LPV system. This approach retains a state-dependent structure while adhering to the LPV framework, enabling the design of effective controllers. Two principal techniques are employed for LPV modeling: the **grid-based approach**, which discretizes the parameter space into points, each associated with a local linear model (Wu 1995; Rugh et al. 2000), and the **polytopic approach**, which combines linear models at specific vertices to approximate the system's behavior as a convex polytope (Apkarian, Gahinet, and Becker 1995). Both techniques facilitate the transformation of a nonlinear system into an LPV framework, enabling the design of controllers that ensure stability and performance across the full range of parameter variations.

3.2.1 Grid-based Model In the grid-based approach, the parameter space is discretized into a grid, where each grid point is associated with a linear model. The selected parameter vector is:

$$\rho = [V_x, V_y, \delta] \quad (6)$$

This choice is specifically made to eliminate non-linearities with respect to state variables, ensuring that the state-space representation reliably captures the vehicle's dynamics under varying conditions. The state-space matrices $A(\rho)$ and $B(\rho)$ are then structured as functions of the parameter vector ρ, and defined as:

$$A(\rho) = \begin{bmatrix} a_{11} & a_{12} & a_{13} \\ 0 & a_{22} & a_{23} \\ 0 & a_{32} & a_{33} \end{bmatrix}, \quad B(\rho) = \begin{bmatrix} b_{11} & b_{12} \\ b_{21} & 0 \\ b_{31} & 0 \end{bmatrix}$$

In this framework, the matrices A and B may incorporate nonlinear functions of the parameter vector ρ. For further details, the explicit elements of these matrices are provided in Appendix A.1.

3.2.2 Polytopic Model The polytopic model represents the system's nonlinear behavior as a convex combination of linear models defined at specific vertices. This approach enables an effective approximation of the system's dynamics across varying conditions by interpolating between these linear models. The general form of the polytopic model is given by:

$$\dot{x}(t) = \sum_{i=1}^{N} \alpha_i(\lambda(t))A_i x(t) + \sum_{i=1}^{N} \alpha_i(\lambda(t))B_i u(t) \quad (7)$$

$$\dot{x}(t) = \underbrace{\begin{bmatrix} \frac{-C_\sigma(.)}{V_x m} & \frac{C_{\alpha f}(.)\delta}{V_x m} & \frac{C_{\alpha f}(.)l_f\delta}{V_x m} + V_y \\ 0 & \frac{-C_{\alpha f}(.) - C_{\alpha r}(.)}{V_x m} & \frac{-C_{\alpha f}(.)l_f + C_{\alpha r}(.)l_r}{V_x m} - V_x \\ 0 & \frac{-C_{\alpha f}(.)l_f + C_{\alpha r}(.)l_r}{V_x I_z} & \frac{-C_{\alpha f}(.)l_f^2 - C_{\alpha r}(.)l_r^2}{V_x I_z} \end{bmatrix}}_{f(x,u)} x(t) + \underbrace{\begin{bmatrix} \frac{-C_{\alpha f}(.)\delta}{m} & \frac{C_\sigma(.)r}{V_x m} \\ \frac{C_{\alpha f}(.)}{m} & 0 \\ \frac{C_{\alpha f}(.)l_f}{I_z} & 0 \end{bmatrix}}_{g(x,u)} u(t) \quad (4)$$

where:

- A_i and B_i are the state-space matrices corresponding to the ith vertex of the polytope.
- $\alpha_i(\lambda)$ are the polytopic coordinates dependent on the parameter vector λ that satisfy the following properties:

$$\sum_{i=1}^{N} \alpha_i(\lambda) = 1, \quad \alpha_i(\lambda) \geq 0 \quad \forall i. \tag{8}$$

For the polytopic representation, the choice of the parameter vector ρ is critical and specific to the chosen system, as it must accurately capture the main non-linearities influencing the vehicle's dynamics. While additional parameters may be available, the selection process focuses on identifying those with the most significant impact on the system's behavior and that can be measured. The polytopic model requires an affine dependence on the parameter vector λ, which as a result includes additional parameters compared to the grid-based approach:

$$\lambda = \left[V_x, \frac{1}{V_x}, V_y, \frac{C_{\alpha f}(V_x)\delta}{V_x}, C_{\alpha f}(V_x), C_{\alpha f}(V_x)\delta \right] \tag{9}$$

where $C_{\alpha f}$ is a nonlinear function of V_x.

The state-space matrices $A(\lambda)$ and $B(\lambda)$ are expressed as affine functions of the chosen parameters. Each matrix at a vertex i of the polytope is defined as:

$$A_i = \begin{bmatrix} a_{11,i} & a_{12,i} & a_{13,i} \\ 0 & a_{22,i} & a_{23,i} \\ 0 & a_{32,i} & a_{33,i} \end{bmatrix}, \quad B_i = \begin{bmatrix} b_{11,i} & b_{12,i} \\ b_{21,i} & 0 \\ b_{31,i} & 0 \end{bmatrix}$$

The elements of the matrices A_i and B_i are functions of the bounds of the parameter vector λ. The specific elements of these matrices are provided in A.2. These matrix elements are evaluated at the vertices of the parameter space, ensuring the system's behavior is accurately represented throughout the operating range. The interpolation coordinates $\alpha_i(\lambda)$ are computed based on the current state and input allowing the combination of the vertex models into a unified polytopic mode.

4. H_∞ CONTROL APPLIED TO LPV SYSTEMS

4.1 Problem Formulation

This section presents the design of an H_∞ controller for LPV systems based on the models developed in Section 3.2, using both grid-based and polytopic approaches.

The scheduling parameters ρ are constrained within predefined intervals that represent realistic operational conditions based on the test platform described in Section 2:

$$\begin{aligned} V_x &\in [0.5\,\text{m/s}, 4\,\text{m/s}], \\ V_y &\in [-0.2\,\text{m/s}, 0.2\,\text{m/s}], \\ \delta &\in [-\frac{\pi}{4}\,\text{rad}, \frac{\pi}{4}\,\text{rad}]. \end{aligned}$$

The primary objectives of the proposed control system are as follows:

- Ensure that the actual yaw rate $\dot{\psi}$, follows the desired yaw rate $\dot{\psi}_{\text{ref}}$, and driving the tracking error to zero.
- Regulate the longitudinal velocity V_x, ensuring it tracks its reference value $V_{x\,ref}$ while maintaining smooth acceleration and deceleration.
- Minimize the lateral velocity V_y, to prevent excessive lateral motion during cornering and other maneuvers.

These control objectives are represented through weighting functions that guide the design of the controller and account for both performance and actuator limitations.

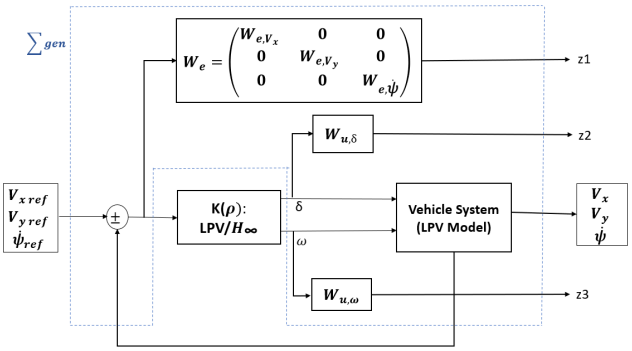

Fig. 3. Generalized plant for control synthesis

The augmented system model, as illustrated in Fig. 3, integrates the LPV model of vehicle dynamics with these weighting functions, leading to the following system formulation:

$$\Sigma_{gen} = \begin{cases} \dot{x}_a(t) = A(\rho)x_a(t) + B_1(\rho)w(t) + B_2(\rho)u(t), \\ z(t) = C_1(\rho)x_a(t) + D_{11}(\rho)w(t) + D_{12}(\rho)u(t), \\ y(t) = C_2(\rho)x_a(t) + D_{21}(\rho)w(t) + D_{22}(\rho)u(t), \end{cases}$$

where $x_a(t)$, $w(t)$, $u(t)$, $z(t)$, and $y(t)$ denote the state vector, references, control input, regulated output and measured output, respectively.

Note that , a constant matrix B_2 is needed for the polytopic approach, first-order filters are introduced to augment the system, as demonstrated in (Apkarian and Gahinet 1995).

The weighting functions as shown in Fig. 3 are designed to achieve desired performance objectives while respecting physical constraints of the system. Since the system is a MIMO system with 2-inputs 3-outputs, the weighting functions are structured as follows:

- $W_{e,*}$: Defines the desired performance for the system's tracking error. The general form is:

$$W_{e,*} = \frac{\frac{s}{M_s} + f_b}{s + f_b\epsilon}$$

  where M_s controls the high-frequency gain, f_b represents the bandwidth of the desired performance, and ϵ is a small parameter to avoid singularities.
- $W_{u,*}$: Penalizes excessive control effort. The general form is

$$W_{u,*} = \frac{s + \frac{f_{bc}}{M_u}}{\epsilon_u s + f_{bc}}$$

  where M_u adjusts the high-frequency gain, f_{bc} represents the bandwidth constraint, and ϵ_u ensures numerical stability.

The specific parameters of these weighting functions chosen for this study are shown in Table 2.

Weight functions	Values
$W_{e,\dot{\psi}}$	$M_s = 2,\ f_b = 2\pi \cdot 0.5\,\text{rad/s},\ \epsilon = 0.01$
W_{e,V_y}	10
$W_{u,\delta}$	$M_u = 1.4,\ f_{bc} = 2\pi \cdot 10\,\text{rad/s},\ \epsilon_u = 0.001$
W_{e,V_x}	$M_s = 2,\ f_b = 2\pi \cdot 0.5\,\text{rad/s},\ \epsilon = 0.01$
$W_{e,\omega}$	$M_u = 150,\ f_{bc} = 2\pi \cdot 10\,\text{rad/s},\ \epsilon_u = 0.001$

Table 2. Chosen weighting parameters.

4.2 LPV/H_∞ Controller Synthesis and analysis

The grid-based and polytopic controllers are synthesized using the H_∞ framework based on Linear Matrix Inequalities (LMIs) (C. Scherer et al. 1997). The objective is to minimize the H_∞ norm of the closed-loop transfer function, ensuring performance across parameter variations. The optimization problem is expressed as:

$$\min_{\mathbf{K}} \gamma \quad \text{subject to} \quad \|T_{\mathbf{K}}\|_\infty \leq \gamma,$$

where $T_{\mathbf{K}}$ represents the closed-loop transfer function and γ is the performance bound to be minimized.

The resulting parameter-dependent controllers $K(\rho)$ are defined as:

$$K(\rho) = \begin{cases} \dot{x}_c(t) = A_c(\rho)x_c(t) + B_c(\rho)y(t), \\ u(t) = C_c(\rho)x_c(t) + D_c(\rho)y(t), \end{cases}$$

where $x_c(t)$ are the controller states, and $A_c(\rho)$, $B_c(\rho)$, $C_c(\rho)$, and $D_c(\rho)$ are parameter-dependent matrices obtained by solving an optimization problem, with the LMIs specifying the constraints of the problem.

Both grid-based and polytopic LPV approaches are considered, ensuring a comprehensive evaluation of their synthesis results. The same weighting functions are applied across both methodologies to ensure a consistent and fair comparison.

Grid-Based Approach The grid-based approach relies here on discretizing the parameter space into $N = 8$ grid points for each parameter, selected to ensure complete coverage of the operational domain while maintaining good performance. This choice allows for accurate modeling of system variations across the parameter range. The LPVTools framework developed by (Hjartarson et al. 2015) was used for controller synthesis, employing parameter-dependent Lyapunov functions to handle the system's variability expressed as:

$$X(\rho) = X_0 + \rho X_1,$$

where X_0 and X_i are constant matrices determined through LMI constraints, and $a_i(\rho)$ are basis functions depending on the varying parameter ρ. The achieved H_∞ performance level of $\gamma = 1.01$ demonstrates performance and control effort minimization all satisfying all design requirements. To further validate the stability of the system, the controller synthesis was tested on a denser grid with 15 points for each parameter. This denser discretization ensures that the stability and performance are maintained over a more refined parameter space.

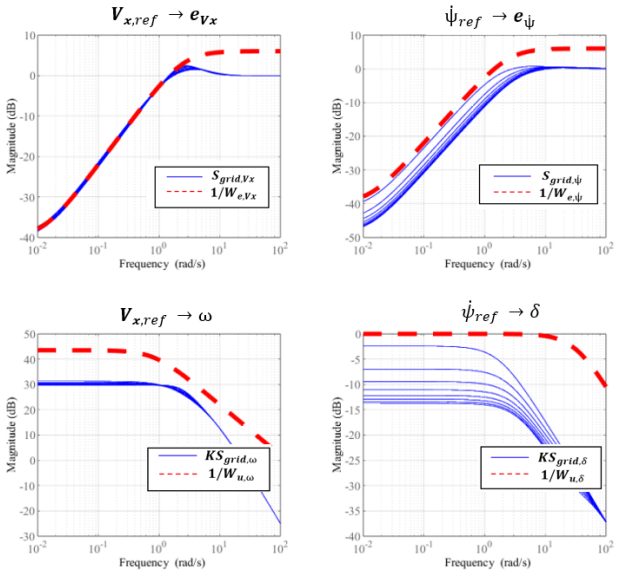

Fig. 4. Comparison of sensitivity S_{grid} and control sensitivity KS_{grid} functions with their respective inverse weighting filters for the grid-based approach.

The grid-based approach provides the sensitivity (S_{grid}) and control sensitivity (KS_{grid}) functions, as shown in Fig. 4. These plots also include the inverse of the weighting functions $1/W_e$ and $1/W_u$, which represent the desired tracking error and control effort constraints, respectively.

From the frequency domain analysis, it can be observed that the sensitivity functions (S_{grid}) remain well below the templates ($1/W_e$) across the entire frequency range. This ensures that the tracking error constraints are satisfied. Similarly, the complementary sensitivity functions (KS_{grid}) are below ($1/W_u$), verifying that the control effort is within the specified limits.

Polytopic approach Following the selection of the parameter vector presented in Equation (9), the polytopic approach represents the LPV system as a hypercube with $2^6 = 64$ vertices. A single, constant Lyapunov function is uniformly applied across all vertices, simplifying the synthesis process while ensuring quadratic stability. The synthesis of the controller matrices at each vertex is carried out by solving an optimization problem using YALMIP (Lofberg 2004) with the solver SeDuMi (Sturm 2024).

For the polytopic approach, the achieved H_∞ performance level is $\gamma = 2.5$, which is more conservative than the grid-based result. This conservatism stems from the large number of vertices in the polytopic model, which may include parameter combinations that do not physically exist. This can be observed in the sensitivity (S_{poly}) and control sensitivity (KS_{poly}) functions shown in Fig. 5, where some plots fail to meet the constraints imposed by the templates ($1/W_e$) and ($1/W_u$), indicating that the tracking error and control effort constraints are not fully satisfied.

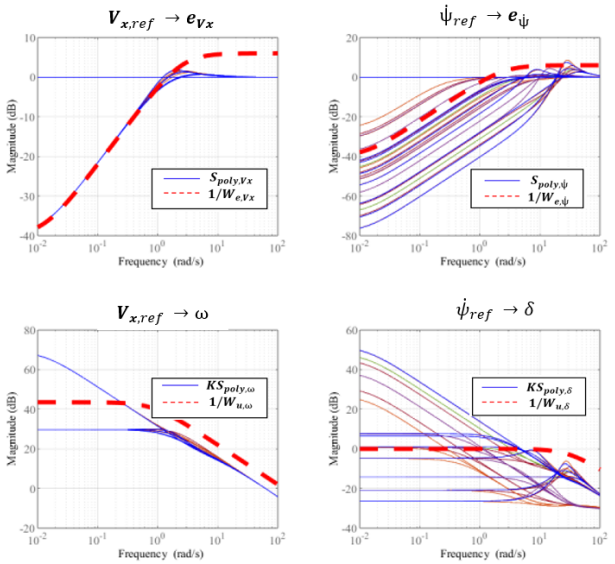

Fig. 5. Comparison of sensitivity S_{poly} and control sensitivity KS_{grid} functions with their respective inverse weighting filters for the polytopic approach

4.3 Discussion and Comparison

A comparison between the two approaches highlights their respective strengths and weaknesses. The grid-based approach achieves a lower γ value (1.01) and better overall performance. This can be attributed to the use of parameter-dependent Lyapunov functions, which enable finer handling of parameter variability. The sensitivity functions for the grid-based controller are closer to the optimal values, demonstrating improved disturbance rejection and reduced control effort. However, the stability in the grid-based approach is only guaranteed at the specific grid points, without explicit guarantees for the regions between these points. To address this limitation, a denser grid was tested to validate the stability of the system within a broader and more refined parameter space. In parallel, the polytopic approach, while achieving a higher γ value (2.5), ensures stability throughout the entire parameter space within the defined hypercube. Additionally, it offers the advantage of reduced computational complexity during the synthesis process. However, this simplification result in a potentially more conservative performance, as evidenced by the higher sensitivity values.

5. SIMULATION RESULTS

This section presents the simulation results to demonstrate the effectiveness of the proposed controllers. A Pure Pursuit algorithm (Ren et al. 2011) was implemented to generate the reference yaw rates ($\dot{\psi}_{\text{ref}}$), and a predefined longitudinal velocity ($V_{x,ref}$) was applied as input. Additionally, a reference of zero for the lateral velocity (V_y) was given in order to minimize the lateral speed. A simulation scenario involving a double lane change was designed to evaluate the performance of the grid-based and polytopic controllers under dynamic driving conditions. This scenario highlights the controllers' ability to handle sudden changes in vehicle dynamics. The results, illustrated in Fig. 6, show that both controllers successfully follow the reference yaw rate. However, the polytopic controller responds slightly faster in tracking $\dot{\psi}_{\text{ref}}$, achieving faster convergence to the reference.

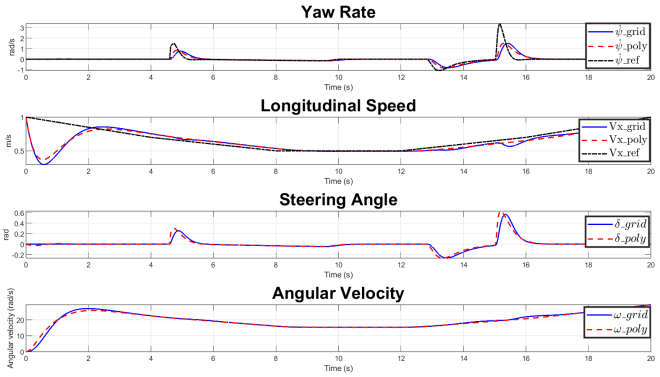

Fig. 6. Comparison of Yaw Rate, Longitudinal Speed, Steering Angle, and Angular Velocity Obtained with Grid-based and Polytopic Approaches

6. PRELIMINARY EXPERIMENTAL TEST RESULTS

This section presents the very recently experimental test results obtained from the implementation of the grid-based controller. A trajectory tracking scenario was performed on the test platform described in Section 2. These experiments aim to validate the practical applicability and effectiveness of the proposed control strategy under real-world conditions. While the testing is still ongoing, initial results provide valuable insights into the controller's performance.

Figure 7 illustrates the results. Subfigure (a) compares the reference and actual vehicle trajectories, showing accurate tracking. Subfigure (b) presents the evolution of yaw rate $\dot{\psi}$, longitudinal velocity V_x, steering angle δ, and angular velocity ω, confirming the controller's stability and responsiveness.

The grid-based controller demonstrates satisfactory performance, successfully tracking the reference trajectory, and minimizing yaw-rate errors. Although minor discrepancies are observed, primarily due to real-world uncertainties and measurement noise, the results validate the controller's effectiveness for trajectory tracking tasks in autonomous vehicle systems. Ongoing tests aim to further refine and assess the controller's performance under varying scenarios and driving conditions. Some implementation refinements were needed to break an algebraic loop arising from the input dependency. This was handled by introducing a one-step delay on the measured scheduling variables, ensuring a causal structure suitable for real-time execution.

7. CONCLUSION

In this paper, an LPV model for the combined longitudinal and lateral dynamics of a small-scale vehicle was developed using both grid-based and polytopic approaches. Based on these models, LPV-H_∞ controllers were designed, and a frequency-domain comparison was performed. Ongoing simulations and real-world tests are being conducted to further validate the performance of the proposed controllers strategies. For future work, it is suggested to

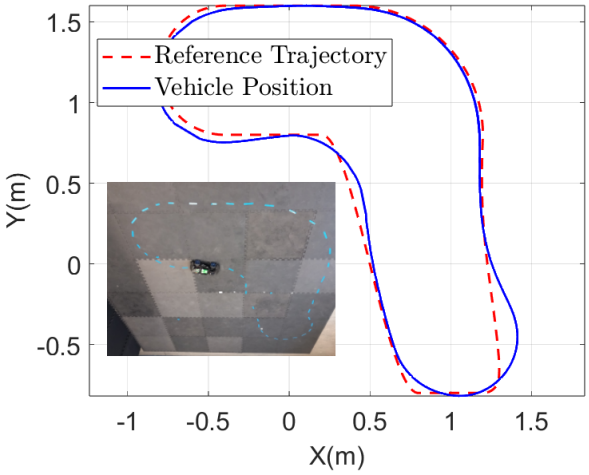

(a) Reference vs actual trajectory.

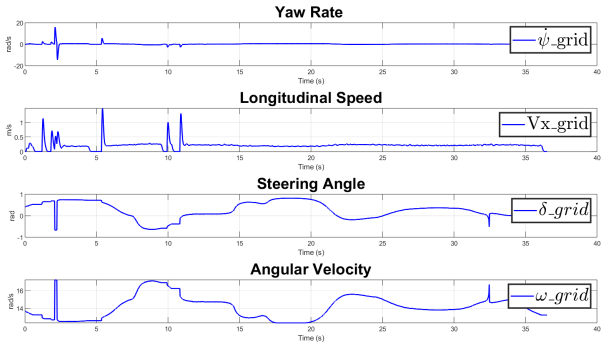

(b) System responses over time.

Fig. 7. Experimental validation of the grid-based controller.

explore different weighting functions for the control synthesis in each approach, tailoring them to improve the performance of each method. Additionally, reducing the polytope for the polytopic approach could help decrease conservatism, leading to more optimal results while maintaining stability guarantees. Furthermore, incorporating actuator modeling and conducting real-world tests for the polytopic approach, which are already underway, will provide a more thorough comparison and validation of the proposed control strategies.

A. APPENDIX

A.1 Matrix elements (grid-based approach)

$$
\begin{aligned}
a_{11} &= \frac{-C_\sigma(\rho_1)}{\rho_1 m}, a_{12} = \frac{C_{\alpha f}(\rho_1)\rho_3}{m\rho_1}, a_{13} = \frac{C_{\alpha f}(\rho_1) l_f \rho_3}{\rho_1 m} + \rho_2,\\
a_{22} &= \frac{-C_{\alpha f}(\rho_1) - C_{\alpha r}(\rho_1)}{\rho_1 m}, a_{23} = \frac{-C_{\alpha f}(\rho_1) l_f + C_{\alpha r}(\rho_1) l_r}{\rho_1 m} - \rho_1,\\
a_{32} &= \frac{-C_{\alpha f}(\rho_1) l_f + C_{\alpha r}(\rho_1) l_r}{\rho_1 I_z}, a_{33} = \frac{-C_{\alpha f}(\rho_1) l_f^2 - C_{\alpha r}(\rho_1) l_r^2}{\rho_1 I_z},\\
b_{11} &= \frac{-C_{\alpha f}(\rho_1)\rho_3}{m}, b_{12} = \frac{C_\sigma(\rho_1) r}{m\rho_1}, b_{21} = \frac{C_{\alpha f}(\rho_1)}{m},\\
b_{31} &= \frac{C_{\alpha f}(\rho_1) l_f}{I_z}
\end{aligned}
$$

A.2 Matrix elements (polytopic approach)

$$
\begin{aligned}
a_{11} &= \frac{-C_\sigma(\rho_1, \rho_2)}{m}, a_{12} = \frac{\rho_4}{m}, a_{13} = \frac{l_f \rho_4}{m} + \rho_3,\\
a_{22} &= \frac{-C_{\alpha f}(\rho_1, \rho_2) - C_{\alpha r}(\rho_1, \rho_2)}{m},\\
a_{23} &= \frac{-C_{\alpha f}(\rho_1, \rho_2) l_f + C_{\alpha r}(\rho_1, \rho_2) l_r}{m} - \rho_1,\\
a_{32} &= \frac{-C_{\alpha f}(\rho_1, \rho_2) l_f + C_{\alpha r}(\rho_1, \rho_2) l_r}{I_z},\\
a_{33} &= \frac{-C_{\alpha f}(\rho_1, \rho_2) l_f^2 - C_{\alpha r}(\rho_1, \rho_2) l_r^2}{I_z}\\
b_{11} &= \frac{-\rho_6}{m}, b_{12} = \frac{C_\sigma(\rho_1, \rho_2) r}{m}, b_{21} = \frac{\rho_5}{m}, b_{31} = \frac{\rho_5 l_f}{I_z}
\end{aligned}
$$

ACKNOWLEDGMENT

This work has been partially supported by ROBOTEX 2.0, the French Infrastructure in Robotics under the grants ROBOTEX (EQUIPEX ANR-10-EQPX-44-01) and TIRREX (EQUIPEX+ grant ANR-21-ESRE-0015).

REFERENCES

Apkarian, P. and R. J. Adams (1998). "Advanced gain-scheduling techniques for uncertain systems". In: *IEEE Transactions on Control Systems Technology* 6.1, pp. 21–32.

Apkarian, P. and P. Gahinet (May 1995). "A convex characterization of gain-scheduled H_∞ controllers". In: *IEEE Transactions on Automatic Control* 40.5, pp. 853–864.

Apkarian, P., P. Gahinet, and G. Becker (1995). "Self-scheduled H_∞ control of linear parameter-varying systems: A design example". In: *Automatica* 31.9, pp. 1251–1261.

Atoui, Hussam (2023). "Switching/Interpolating LPV Control based on Youla-Kucera Parameterization: application to Autonomous Vehicles". PhD thesis. Université Grenoble Alpes.

Blanchini, F. et al. (2000). "Set-theoretic methods in robust control". In: *Automatica* 37.1, pp. 3–19.

C. Scherer, P. Gahinet et al. (1997). "Multiobjective output-feedback control via LMI optimization," in: *in IEEE Transactions on Automatic Control, vol. 42, no. 7, pp. 896-911.*

Doumiati, Moustapha et al. (2013). "Integrated vehicle dynamics control via coordination of active front steering and rear braking". In: *European Journal of Control* 19.2, pp. 121–143.

Fergani, S. et al. (2016). "LPV/H suspension robust control adaption of the dynamical lateral load transfers based on a differential algebraic estimation approach". In: *IFAC-PapersOnLine* 49.11, pp. 440–447.

Hjartarson, Arnar et al. (2015). "LPVTools: A Toolbox for Modeling, Analysis, and Synthesis of Parameter Varying Control Systems". In: *IFAC-PapersOnLine* 48.26. 1st IFAC Workshop on Linear Parameter Varying Systems LPVS 2015, pp. 139–145.

Hoffmann, C. et al. (Mar. 2015). "A survey of linear parameter-varying control applications validated by experiments or high-fidelity simulations". In: *IEEE Transactions on Control Systems Technology* 23.2, pp. 416–433.

Jazar, Reza N. (2017). *Vehicle Dynamics*. Cham: Springer International Publishing.

Kapsalis, Dimitrios (2022). "LPV/Gain-Scheduled lateral control architectures for autonomous vehicles". PhD thesis. Université Grenoble Alpes.

Kiencke, U. et al. (2005). *Automotive control systems: for engine, driveline, and vehicle*. 2nd ed. Springer. 512 pp.

Leith, D. J. et al. (Dec. 2000). "On Formulating Nonlinear Dynamics in LPV Form". In: *Proceedings of the 39th IEEE Conference on Decision and Control*, pp. 3526–3527.

Li, Zihan et al. (2021). "Coordinated longitudinal and lateral vehicle stability control based on the combined-slip tire model in the MPC framework". In: *Mechanical Systems and Signal Processing.*

Liu, Hanghang et al. (2024). “NMPC-driven enhancement of vehicle chassis stability: Unified approach to lateral, longitudinal, and vertical dynamics”. In: *Transportation Engineering*.

Lofberg, Johan (2004). “YALMIP: A toolbox for modeling and optimization in MATLAB”. In: *Computer Aided Control Systems Design, 2004 IEEE International Symposium on*. IEEE, pp. 284–289.

Medero Borrell, Ariel (2023). “LPV lateral control of autonomous and automated vehicles”. PhD thesis. Universitat Politècnica de Catalunya,Université Grenoble Alpes.

Pacejka, Hans B (2006). *Tyre and Vehicle Dynamics*. Butterworth-Heinemann,Elsevier.

Penco, Dario (2022). “Contrôle véhicule autonome. Contrôle robuste et haute performance pour permettre les manœuvres à haute dynamique des véhicules autonomes”. PhD thesis. Université Paris-Saclay, CentraleSupélec.

Ren, DianBo et al. (2011). “Trajectory Planning and Yaw Rate Tracking Control for Lane Changing of Intelligent Vehicle on Curved Road”. In: *Science China Technological Sciences* 54.2, pp. 307–320.

Rugh, Wilson J. et al. (2000). “Research on gain scheduling”. In: *Automatica* 36.10, pp. 1401–1425.

Sename, O. et al. (2013). *Robust Control and Linear Parameter Varying Approaches*. Springer.

Slotine, J.-J. E. et al. (1991). *Applied Nonlinear Control*. Prentice Hall.

Sturm, Jos F. (2024). *SeDuMi: A software package for solving optimization problems over symmetric cones*. Ed. by Computational Optimization Research at Lehigh (COR@L).

Teng, Fei et al. (2024). “Cooperative control strategy of trajectory tracking and driving stability for distributed-drive vehicles under extreme conditions”. In: *Control Engineering Practice* 147, p. 105905.

Toth, Roland (2010). *Modeling and Identification of Linear Parameter-Varying Systems*. Vol. 403. Springer Science & Business Media.

Wu, F. (1995). “Control of Linear Parameter Varying Systems”. PhD thesis. Berkeley, CA, USA: University of California, Berkeley.